IOP PUBLISHING CLASSICAL AND QUANTUM GRAVITY

Class. Quantum Grav. **27** (2010) 045012 (15pp) doi:10.1088/0264-9381/27/4/045012

Black objects and hoop conjecture in five-dimensional space-time

Yuta Yamada and Hisa-aki Shinkai

Faculty of Information Science and Technology, Osaka Institute of Technology, 1-79-1 Kitayama, Hirakata, Osaka 573-0196, Japan

E-mail: m1m08a26@info.oit.ac.jp and shinkai@is.oit.ac.jp

Received 25 September 2009, in final form 29 December 2009
Published 29 January 2010
Online at stacks.iop.org/CQG/27/045012

Abstract

We numerically investigated the sequences of initial data of a thin spindle and a thin ring in five-dimensional space-time in the context of the cosmic censorship conjecture. We modeled the matter in non-rotating homogeneous spheroidal or toroidal configurations under the momentarily static assumption, solved the Hamiltonian constraint equation and searched the apparent horizons. We discussed when S^3 (black-hole) or $S^1 \times S^2$ (black-ring) horizons ('black objects') are formed. By monitoring the location of the maximum Kretchmann invariant, an appearance of 'naked singularity' or 'naked ring' under special situations is suggested. We also discuss the validity of the *hyper-hoop* conjecture using a minimum *area* around the object, and show that the appearance of the ring horizon does not match with this hoop.

PACS numbers: 04.20.Dw, 04.20.Ex, 04.25.dc, 04.50.Gh

(Some figures in this article are in colour only in the electronic version)

1. Introduction

In general relativity, there are two famous conjectures concerning the gravitational collapse. One is the cosmic censorship conjecture [1] which states that collapse driven singularities will always be clothed by an event horizon and hence can never be visible from the outside. The other is the hoop conjecture [2] which states that black holes will form when and only when a mass M gets compacted into a region whose circumference C in every direction is $C \leqslant 4\pi M$. These two conjectures have been extensively studied in various methods; among them we believe that the numerical works by Shapiro and Teukolsky [3] showed the most exciting results: (a tendency of) the appearance of a naked singularity. This was reported from the fully relativistic time evolution of collisionless particles in a highly prolate initial shape;

and the results of time evolutions are in agreement with the predictions of the sequence of their initial data [4].

In recent years, on the other hand, gravitation in higher dimensional space-time is getting a lot of attention. This is from an attempt to unify fundamental forces including gravity at TeV scale, and if so, it is suggested that small black holes might be produced at the CERN large hadron collider (LHC). The LHC experiments are expected to validate several higher dimensional gravitational models. In such an exciting situation, the theoretical interests are also in the general discussion of black-hole structures. Our discussion is one of them: in what circumstances are black holes formed?

New features of higher dimensional black holes and black objects are reported due to additional physical freedoms. The four-dimensional black holes are known to be S^2 from the topological theorem. Also in the asymptotically flat and stationary space-time, four-dimensional black holes are known to be the Kerr black hole from the uniqueness theorem. On the other hand, in higher dimensional space-time, quite rich structures are available, such as a torus black hole ('black ring') with $S^1 \times S^2$ horizon [5, 6] or black Saturn [7], black di-ring [8, 9] (see the review [10] for references). The uniqueness theorem of axisymmetric space-time in a higher dimension is known to be violated.

So far, the black-hole studies in higher dimensional space-time are mainly carried out using analytic stationary solutions. There are also many numerical attempts to seek the higher dimensional black-hole structures, e.g. collider-oriented dynamical features [11, 12], a new stationary solution sequence [13], (here we selected the works with asymptotically flat space-time). However, fully relativistic dynamical features, such as the formation processes, stabilities and late-time fate of the black objects, are left unknown. We plan to investigate such dynamical processes numerically, and this is the first report on the constructions of the sequences of initial data for time evolution.

The hoop conjecture tries to denote 'if' and 'only if' conditions for the formation of the horizon in the process of gravitational collapse. The 'only if' part of the statement would be replaced with the so-called Gibbons–Penrose isoperimetric inequality [14], $M \geqslant \sqrt{A/16\pi}$, where M is the total mass and A is the area of the trapped surface. This inequality is based on the cosmic censorship conjecture, so that its proof or disproof is the important issue (see a precise formulation in [15] and a recent review [16]).

The higher dimensional versions of the hoop conjecture and the isoperimetric inequality have been discussed so far [17, 19–21]. While there are differences in their coefficiencies, the hoop conjecture in D-dimensional space-time would be basically expressed as follows: a black hole with horizons form when and only when a mass M gets compacted into a region whose $(D-3)$-dimensional area V_{D-3} in every direction is

$$V_{D-3} \leqslant G_D M, \tag{1}$$

where G_D is the gravitational constant in D-dimensional theory of gravity. Here V_{D-3} means the volume of $(D-3)$-dimensional closed submanifold of a space-like hypersurface. That is, the hoop C in four-dimensional space-time is replaced with the *hyper-hoop* V_{D-3}; if $D = 5$, then the *hyper-hoop* would be an area V_2. However, in five-dimensional space-time, black holes are not restricted to have a simply connected horizon; therefore, the applicabilities of the hyper-hoop and the isoperimetric inequality to various black objects are left unknown. The validity of (1) was investigated in several idealized models by Ida and Nakao [17] and Yoo *et al* [18], who solved momentarily static, conformally flat, five-dimensional axisymmetric homogeneous spheroidal matter and δ-function-type ring matter. Our purpose is to investigate the generality of the hyper-hoop conjecture and the cosmic censorship conjecture in more general situations.

In this paper, we present two kinds of initial data; spheroidal and toroidal matter configurations. We solve the Hamiltonian constraint equation numerically, and then search apparent horizons. This study is the generalization of [17, 18]; we reproduce their results as our code checks, and present also finite-sized ring cases. The definition of the hyper-hoop is not yet definitely given in the community, so that we propose to define the hyper-hoop as a local minimum of the area by solving the Euler–Lagrange-type equation.

This paper is organized as follows. In the next section, we explain how to set initial data for five-dimensional space-time and how to search S^3 and $S^1 \times S^2$ apparent horizons and hoops. In section 3, we show numerical results. The final section is devoted to the summary and discussion. We use the unit $c = 1$ and $G_5 = 1$, where c is the speed of light and G_5 is the gravitational constant of the five-dimensional space-time.

2. Basic equations and numerical issues

2.1. The Hamiltonian constraint equation

We consider the initial data sequences on a four-dimensional space-like hypersurface. A solution of the Einstein equations is obtained by solving the Hamiltonian constraint equation if we assume the moment of time symmetry. We apply the standard conformal approach [22] to obtain the four-metric γ_{ij}. As was discussed in [23], in $4+1$ space-time decomposition, the equations would be simplified with a conformal transformation

$$\gamma_{ij} = \psi^2 \hat{\gamma}_{ij}, \tag{2}$$

where $\hat{\gamma}_{ij}$ is the trial base metric which we assume conformally flat:

$$\mathrm{d}s^2 = \hat{\gamma}_{ij}\,\mathrm{d}x^i \mathrm{d}x^j = \mathrm{d}x^2 + \mathrm{d}y^2 + \mathrm{d}z^2 + \mathrm{d}w^2. \tag{3}$$

The Hamiltonian constraint equation, then, becomes

$$\hat{\Delta}\psi = -4\pi^2 G_5 \rho, \tag{4}$$

where ρ is the effective Newtonian mass density and G_5 is the gravitational constant in five-dimensional theory of gravity. We numerically solve equation (4) in the upper-half coordinate region ($x \geqslant 0$, $y \geqslant 0$, $z \geqslant 0$, $w \geqslant 0$) with setting the boundary conditions as

$$\nabla\psi = 0 \quad \text{(at inner boundaries)}, \tag{5}$$

and

$$\psi = 1 + \frac{M_{\mathrm{ADM}}}{r^2} \quad \text{(at outer boundaries)}, \tag{6}$$

where

$$r = \sqrt{x^2 + y^2 + z^2 + w^2} \tag{7}$$

and M_{ADM} can be interpreted as the ADM mass of the matter. Practically, the boundary condition, (6), is replaced with

$$(\psi - 1)r^2 = \text{const.} \tag{8}$$

and we apply

$$\frac{\partial}{\partial x^i}[(\psi - 1)r^2] = 0 \tag{9}$$

on the outer edge of our numerical grid. The ADM mass M_{ADM}, then, is evaluated from equation (6).

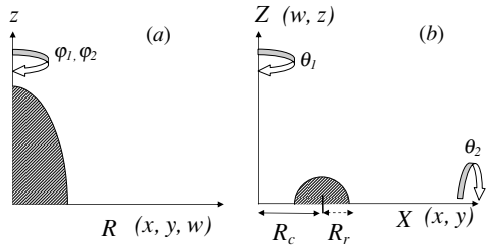

Figure 1. Axis of symmetry of our models: (*a*) spheroidal (spindle) configuration, and (*b*) toroidal configuration. We consider the matter with uniform density. We adopt the coordinate as equation (10) for case (*a*), while we use equation (11) for case (*b*).

As is described below, we consider two models of the matter distribution: spheroidal and toroidal configurations. By assuming the axis of symmetry, both are reduced to effectively two-dimensional problems (figure 1). For the spheroidal matter (figure 1(*a*)), we use the metric

$$ds^2 = \psi(R, z)^2 \left[dR^2 + R^2\left(d\varphi_1^2 + \sin^2\varphi_1\, d\varphi_2^2\right) + dz^2\right] \tag{10}$$

where

$$R = \sqrt{x^2 + y^2 + z^2}, \qquad \varphi_1 = \tan^{-1}\left(\frac{w}{\sqrt{x^2 + y^2}}\right) \qquad \text{and} \qquad \varphi_2 = \tan^{-1}\left(\frac{y}{x}\right).$$

For the toroidal case (figure 1(*b*)), on the other hand, we use the metric

$$ds^2 = \psi(X, Z)^2(dX^2 + dZ^2 + X^2\, d\vartheta_1 + Z^2\, d\vartheta_2) \tag{11}$$

where

$$X = \sqrt{x^2 + y^2}, \qquad Z = \sqrt{z^2 + w^2},$$
$$\vartheta_1 = \tan^{-1}\left(\frac{y}{x}\right), \qquad \text{and} \qquad \vartheta_2 = \tan^{-1}\left(\frac{z}{w}\right).$$

By assuming that φ_1 and φ_2 (ϑ_1 and ϑ_2 for the toroidal case) are the angles around the axis of symmetry, the Hamiltonian constraint equation, (4), effectively becomes

$$\frac{\partial^2\psi}{\partial R^2} + \frac{2}{R}\frac{\partial\psi}{\partial R} + \frac{\partial^2\psi}{\partial z^2} = -4\pi^2 G_5\rho, \tag{12}$$

and

$$\frac{1}{X}\frac{\partial}{\partial X}\left(X\frac{\partial\psi}{\partial X}\right) + \frac{1}{Z}\frac{\partial}{\partial Z}\left(Z\frac{\partial\psi}{\partial Z}\right) = -4\pi^2 G_5\rho, \tag{13}$$

respectively. We solve (12) and (13) using the normal successive over-relaxation (SOR) method with red–black ordering. We use 500^2 grids for the range (R, z) or $(X, Z) = [0, 10]$ with the tolerance 10^{-6} for ψ for solving equations (12) and (13). The presenting results are the sequences of the constant $M_{\rm ADM}$ within the error $O(10^{-2})$.

2.2. Matter distributions

We model the matter by non-rotating homogeneous spheroidal and toroidal configurations with effective Newtonian uniform mass density. Our first model is the case with homogeneous

spheroidal matter, which is expressed as

$$\frac{x^2}{a^2}+\frac{y^2}{a^2}+\frac{w^2}{a^2}+\frac{z^2}{b^2}\leqslant 1, \tag{14}$$

where a and b are parameters. This is the $(4+1)$-dimensional version of the earlier study of Nakamura *et al* [4], and also the numerical reproduction of Ida and Nakao [17] and Yoo *et al* [18]. The second is the case with homogeneous toroidal matter configurations, described as

$$\left(\sqrt{x^2+y^2}-R_c\right)^2+\left(\sqrt{w^2+z^2}\right)^2\leqslant R_r^2, \tag{15}$$

where R_c is the circle radius of torus, and R_r is the ring radius (figure 1(*b*)). This case is motivated from the 'black-ring' solution [5] though not including any rotations of matter nor of the space-time. Nevertheless, we consider this is the first step for toroidal configuration, since this is the generalization of [17] to the finite-sized matter cases.

2.3. Kretchmann invariant

After obtaining the initial data, we evaluate the Kretchmann invariant

$$\mathcal{I}^{(4)}=R_{abcd}R^{abcd}, \tag{16}$$

where R_{abcd} is the four-dimensional Riemann tensor, in order to measure the strength of gravity. This is most easily evaluated in Cartesian coordinates as

$$\begin{aligned}\mathcal{I}^{(4)}=16\sum_{i\neq j}\left[2\left(\frac{\partial\psi}{\partial x^i}\right)\left(\frac{\partial\psi}{\partial x^j}\right)-\psi\frac{\partial^2\psi}{\partial x^i\partial x^j}\right]^2\\ +8\sum_{i\neq j}\left[\left(\frac{\partial\psi}{\partial x^i}\right)^2-\left(\frac{\partial\psi}{\partial x^j}\right)^2\right]^2+4\psi^2\sum_{i\neq j}\left[\frac{\partial^2\psi}{\partial {x^i}^2}+\frac{\partial^2\psi}{\partial {x^j}^2}\right]^2\\ +8\psi\left[\sum_i\left(\frac{\partial\psi}{\partial x^i}\right)^2\right]\left[\sum_i\frac{\partial^2\psi}{\partial {x^i}^2}\right]-32\psi\sum_i\left(\frac{\partial\psi}{\partial x^i}\right)^2\left(\frac{\partial^2\psi}{\partial {x^i}^2}\right).\end{aligned}$$

2.4. Apparent horizons

For investigating the validity of the censorship conjecture and hyper-hoop conjecture, we search the existence of apparent horizons. An apparent horizon is defined as a marginally outer trapped surface, and the existence of the apparent horizon is the sufficient condition for the existence of the event horizon. On the four-dimensional space-like hypersurface, an apparent horizon is a three-dimensional closed marginal surface.

In order to locate the apparent horizon for the spheroidal configurations, after obtaining the solution of (12), we transform the coordinate from (R, z) to (r, θ), using

$$r=\sqrt{R^2+z^2}, \tag{17}$$

$$\theta=\tan^{-1}\left(\frac{R}{z}\right), \tag{18}$$

and search the apparent horizon on the R-z section [17, 18]. The location of the apparent horizon, $r_M(\theta)$, is identified by solving

$$\begin{aligned}\ddot{r}_M-\frac{4\dot{r}_M^2}{r_M}-3r_M+\frac{r_M^2+\dot{r}_M^2}{r_M}\left[\frac{2\dot{r}_M}{r_M}\cot\theta-\frac{3}{\psi}(\dot{r}_M\sin\theta+r_M\cos\theta)\frac{\partial\psi}{\partial z}\right.\\ \left.+\frac{3}{\psi}(\dot{r}_M\cos\theta-r_M\sin\theta)\frac{\partial\psi}{\partial R}\right]=0,\end{aligned} \tag{19}$$

where dot denotes θ-derivative. We solve (19) for $r_M(\theta)$ using the Runge–Kutta method starting on the z-axis ($\theta = 0$) with a trial value $r = r_0$ and integrate to $\theta = \pi/2$, with interpolating the coefficients ψ and $\frac{\partial\psi}{\partial x^i}$ from the data on the grid points. We apply the symmetric boundary condition on the both ends. If there is no solution satisfying both boundary conditions, we judge there is no horizon.

For toroidal cases, we transform the coordinate from (X, Z) to (r, ϕ), using

$$r = \sqrt{X^2 + Z^2}, \qquad \text{and} \qquad \phi = \tan^{-1}\left(\frac{Z}{X}\right). \tag{20}$$

The location of the apparent horizon, $r_m(\phi)$, is then identified by solving

$$\ddot{r_m} - 4\frac{\dot{r_m}^2}{r_m} - 3r_m - \frac{r_m^2 + \dot{r_m}^2}{r_m}\left[2\frac{\dot{r_m}}{r_m}\cot(2\phi) - \frac{3}{\psi}(\dot{r_m}\sin\phi + r\cos\phi)\frac{\partial\psi}{\partial X} + \frac{3}{\psi}(\dot{r_m}\cos\phi - r_m\sin\phi)\frac{\partial\psi}{\partial Z}\right] = 0, \tag{21}$$

with the symmetric boundary condition $\dot{r} = 0$ at both $\phi = 0$ and $\pi/2$. When the matter is in torus shape, an additional $S^1 \times S^2$ apparent(ring horizon) horizon may exist. In order to find a ring horizon, we adopt the coordinate as

$$r = \sqrt{(X - R_c)^2 + Z^2}, \qquad \text{and} \qquad \xi = \tan^{-1}\left(\frac{Z}{X - R_c}\right). \tag{22}$$

This marginal surface is obtained by solving the equation for $r(\xi)$:

$$\ddot{r_m} - \frac{3\dot{r_m}^2}{r_m} - 2r_m - \frac{r_m^2 + \dot{r_m}^2}{r_m} \times \left[\frac{\dot{r_m}\sin\xi + r_m\cos\xi}{r_m\cos\xi + R_c} - \frac{\dot{r_m}}{r_m}\cot\xi + \frac{3}{\psi}(\dot{r_m}\sin\xi + r\cos\xi)\frac{\partial\psi}{\partial x} - \frac{3}{\psi}(\dot{r_m}\cos\xi - r\sin\xi)\frac{\partial\psi}{\partial z}\right] = 0, \tag{23}$$

where dot denotes ξ-derivative, with the symmetric boundary condition on the both ends at $\xi = 0$ and π.

2.5. Area of horizons

From the obtained sequence of initial data, we calculate the surface area A_3 of the apparent horizons. If the obtained horizon is spheroidal configuration, the surface area of the horizon, A_3, becomes

$$A_3^{(S)} = 8\pi \int_0^{\pi/2} \psi^3 r_M^2 \sin^2\theta \sqrt{\dot{r_M}^2 + r_M^2}\, \mathrm{d}\theta, \tag{24}$$

where dot denotes a θ-derivative. As for the toroidal cases, the surface area of S^3 and $S^1 \times S^2$ apparent horizons become

$$A_3^{(T1)} = 4\pi^2 \int_0^{\pi/2} \psi^3 r_m^2 \cos\phi \sin\phi \sqrt{\dot{r_m}^2 + r_m^2}\, \mathrm{d}\phi, \tag{25}$$

and

$$A_3^{(T2)} = 4\pi^2 \int_0^{\pi} \psi^3 (R_c + r_m\cos\xi) r_m \sin\xi \sqrt{\dot{r_m}^2 + r_m^2}\, \mathrm{d}\xi, \tag{26}$$

where dot denotes a ϕ-derivative and a ξ-derivative, respectively.

2.6. Hyper-hoop

We also calculate the hyper-hoop for the five-dimensional hoop-conjecture which is defined by a two-dimensional area. We try to verify the necessary condition of the black-hole formation examined in [18]:

$$V_2 \leqslant \frac{\pi}{2} 16\pi G_5 M. \tag{27}$$

However, the definition of V_2 is not so far defined apparently. We, therefore, propose to define the hoop V_2 as a surrounding two-dimensional area which satisfies the local minimum area condition,

$$\delta V_2 = 0. \tag{28}$$

When the area of the space-time outside the matter is expressed by a coordinate r, then equation (28) leads to the Euler–Lagrange-type equation for $V_2(r, \dot{r})$.

For the spheroidal configuration, we express the area V_2 using $r = r_h(\theta)$ as

$$V_2^{(A)} = 4\pi \int_0^{\pi/2} \psi^2 \sqrt{\dot{r_h}^2 + r_h^2}\, r_h \sin\theta \, \mathrm{d}\theta, \tag{29}$$

or

$$V_2^{(B)} = 4\pi \int_0^{\pi/2} \psi^2 \sqrt{\dot{r_h}^2 + r_h^2}\, r_h \cos\theta \, \mathrm{d}\theta, \tag{30}$$

where dot denotes a θ-derivative. $V_2^{(A)}$ expresses the surface area which is obtained by rotating with respect to the z-axis, while $V_2^{(B)}$ is the one with R-axis rotation. Then the hyper-hoop $V_2^{(A)}$ is derived by

$$\ddot{r_h} - \frac{3\dot{r_h}^2}{r_h} - 2r_h + \frac{r_h^2 + \dot{r_h}^2}{r_h}\left[\frac{\dot{r_h}}{r_h}\cot\theta - \frac{2}{\psi}(\dot{r_h}\sin\theta + r_h\cos\theta)\frac{\partial\psi}{\partial z} - \frac{2}{\psi}(r_h\sin\theta - \dot{r_h}\cos\theta)\frac{\partial\psi}{\partial R}\right] = 0, \tag{31}$$

while the hyper-hoop $V_2^{(B)}$ is derived by

$$\ddot{r_h} - \frac{3\dot{r_h}^2}{r_h} - 2r_h - \frac{r_h^2 + \dot{r_h}^2}{r_h}\left[\frac{\dot{r_h}}{r_h}\tan\theta + \frac{2}{\psi}(r_h\sin\theta - \dot{r_h}\cos\theta)\frac{\partial\psi}{\partial R} + \frac{2}{\psi}(r_h\cos\theta + \dot{r_h}\sin\theta)\frac{\partial\psi}{\partial z}\right] = 0. \tag{32}$$

We search the location of the minimum V_2 by solving (31) and (32), applying the same technique and the boundary conditions with those of horizons.

For the toroidal cases, the hoop is expressed using $r = r_h(\phi)$ as

$$V_2^{(C)} = 4\pi \int_0^{\pi/2} \psi^2 \sqrt{\dot{r_h}^2 + r_h^2}\, r_h \cos\phi \, \mathrm{d}\phi, \tag{33}$$

or

$$V_2^{(D)} = 4\pi \int_0^{\pi/2} \psi^2 \sqrt{\dot{r_h}^2 + r_h^2}\, r_h \sin\phi \, \mathrm{d}\phi. \tag{34}$$

$V_2^{(C)}$ expresses the surface area which is obtained by rotating with respect to the z-axis, while $V_2^{(D)}$ is the one with x-axis rotation. Then, the minimum $V_2^{(C)}$ satisfies the equation

$$\ddot{r_h} - \frac{3\dot{r_h}^2}{r_h} - 2r_h + \frac{r_h^2 + \dot{r_h}^2}{r_h}\left[\frac{\dot{r_h}}{r_h}\cot\phi - \frac{2}{\psi}(\dot{r_h}\sin\phi + r_h\cos\phi)\frac{\partial\psi}{\partial X} - \frac{2}{\psi}(r_h\sin\phi - \dot{r_h}\cos\phi)\frac{\partial\psi}{\partial Z}\right] = 0, \tag{35}$$

and $V_2^{(D)}$ satisfies

$$\ddot{r}_h - \frac{3\dot{r}_h^2}{r_h} - 2r_h - \frac{r_h^2 + \dot{r}_h^2}{r_h}\left[\frac{\dot{r}_h}{r_h}\tan\phi + \frac{2}{\psi}(r_h \sin\phi - \dot{r}_h \cos\phi)\frac{\partial\psi}{\partial X} + \frac{2}{\psi}(r_h \cos\phi + \dot{r}_h \sin\phi)\frac{\partial\psi}{\partial Z}\right] = 0. \tag{36}$$

We also calculate the hyper-hoop with $S^1 \times S^1$ topology for the toroidal cases, $V_2^{(E)}$,

$$V_2^{(E)} = 2\pi \int_0^\pi \psi^2 \sqrt{\dot{r}_h^2 + r_h^2}(r_h \cos\xi + R_c)\,\mathrm{d}\xi. \tag{37}$$

The minimum $V_2^{(E)}$ satisfies the equation

$$\ddot{r}_h - \frac{3\dot{r}_h^2}{r_h} - 2r_h - \frac{r_h^2 + \dot{r}_h^2}{r_h}\left[\frac{-R_c + \dot{r}_h \sin\xi}{R_c + r_h \cos\xi} + \frac{2}{\psi}(\dot{r}_h \sin\xi + r_h \cos\xi)\frac{\partial\psi}{\partial X} + \frac{2}{\psi}(r_h \sin\xi - \dot{r}_h \cos\xi)\frac{\partial\psi}{\partial Z}\right] = 0. \tag{38}$$

3. Numerical results

3.1. Spheroidal configurations

First, we show the cases with spheroidal matter configurations. In figure 2, we display matter distributions and the shape of the apparent horizon (if it exists). When the matter is spherical, $a = b$ (the cases of (a), (d) in figure 2), the horizon is also spherically symmetric and locates at the Schwarzschild radius, r_s. The horizon becomes prolate as the value b/a increases. We cannot find the apparent horizon when length b is larger than $b = 1.5$ for $a = 0.5$ and $b = 2.0$ for $a = 0.1$. We see from (b) and (e) of figure 2 that the matter configurations can be arbitrarily large but the apparent horizon does not cover all the matter regions. This behavior is the same with $(3 + 1)$-dimensional cases [4] and our numerical results reproduce the results in [18]. If we compare our five-dimensional results with four-dimensional ones [4], the disappearance of the apparent horizon can be seen only for the highly prolate cases. (For example, for the eccentricity 0.999 cases, the disappearance of the apparent horizon starts at the prolate radius 0.7 M in the four-dimensional case, while 2.0 r_s in our case.) Therefore, we expect that an appearance of a singular behavior is 'relaxed' in a five-dimensional case, and this tendency would be the same for the higher dimensional cases.

The asterisk in figure 2 is the location of the largest Kretchmann invariant, $\mathcal{I}_{\max} = \max\{R^{(4)}_{abcd}R^{(4)abcd}\}$. For all cases, we see that the locations of $\mathcal{I}_{\max}$ are always outside the matter, except the cases of $b = a$.[1] We show the contours of $\mathcal{I}^{(4)}$ in figure 3. Figure 4 display $\mathcal{I}_{\max}$ as a function of b/a. We see that $\mathcal{I}_{\max}$ monotonically increases even if there is no apparent horizon. In the $(3+1)$-dimensional cases, the extremely elongated spindle evolves into a naked singularity [4]. Our results suggest such evolutions also in the $(4+1)$-dimensional cases.

In figure 5, we show the surface area of the apparent horizon A_3. We observe that A_3 becomes the largest when the matter is spherical. If we took into account the analogy of the thermodynamics of the black hole, this may suggest that the final state of the 5D black hole shakes down to spherically symmetric.

[1] The Kretchmann invariant expresses the strength of the curvature, which is determined by the gradient of the metric. For example, when we solve a single star with uniform density, the maximum value of the metric appears at the center of matter configuration, but the maximum value of the metric gradient appears off-center and likely at the outside of the matter region. Therefore, our results of the location of the maximum Kretchmann invariant are not strange.